A space-time BIE method for nonhomogeneous exterior wave equation problems. the Dirichlet case

A space-time BIE method for non homogeneous exterior wave equation problems. The Dirichlet case. *

S. Falletta†, G. Monegato‡, L. Scuderi§

This is the authors' post-print version of an article published on *IMA Journal of Numerical Analysis*, Volume 32, Number 1 (2012), pp. 202-226, DOI: 10.1093/imanum/drr008.¶

To the memory of James N. Lyness

Abstract

In this paper we consider the (2D and 3D) exterior problem for the non homogeneous wave equation, with a Dirichlet boundary condition and non homogeneous initial conditions. First we derive two alternative boundary integral equation formulations to solve the problem. Then we propose a numerical approach for the computation of the extra "volume" integrals generated by the initial data. To show the efficiency of this approach, we solve some test problems by applying a second order Lubich discrete convolution quadrature for the discretization of the time integral, coupled with a classical collocation boundary element method. Some conclusions are finally drawn.

KEY WORDS: wave equation; non homogeneous conditions; space-time boundary integral equations; numerical methods

1 Introduction

Boundary integral equation formulations for elliptic problems is nowadays a well established and studied tool for solving such problems. This is not the case for time dependent problems, namely parabolic and hyperbolic problems. In particular, although space-time boundary integral formulations have been used for many years by

*This work was supported by the Ministero dell'Istruzione, dell'Università e della Ricerca of Italy, under the research program PRIN07: Boundary element methods for time-dependent problems.

†Dipartimento di Matematica, Politecnico di Torino, Italy. Email: silvia.falletta@polito.it

‡Dipartimento di Matematica, Politecnico di Torino, Italy. Email: giovanni.monegato@polito.it

§Dipartimento di Matematica, Politecnico di Torino, Italy. Email: letizia.scuderi@polito.it

engineers to solve such problems, the development of a satisfactory theory and of standard numerical tools for their solution is still far from being satisfactory. For a survey on this topic see for example [11].

In the case of the exterior problem for the homogeneous wave equation, with homogeneous initial conditions, some fundamental theoretical results have been derived in [6], [7] in 1986. Later, in 1994, starting from these results, Lubich in [22] proposed and examined a new numerical approach to solve such problems when the boundary condition is the Dirichlet one. His method is based on a special (convolution) quadrature rule (see [21], [27]) he has constructed and examined, for the discretization of the time integral, and of a standard Galerkin BEM for the space integration. For his numerical scheme he has proved unconditional stability and convergence. In 2009 this theory has been extended and developed also for the Neumann problem [9]. Lubich's approach has been also used to solve some homogeneous wave propagation problems in elastodynamics (see, for example, [28],[18],[32]).

Very recently, Lubich's paper has stimulated the study of some fast algorithms for the implementation of the convolution quadrature/Galerkin method (see for example [8], [16]), which take into account the lower block triangular Toeplitz structure of the final linear system and the behavior of its matrix elements.

However, except for a few papers written by engineers (see for example [24], [3], [2]), none of the above mentioned papers deals with the non homogeneous wave equation with non homogeneous initial conditions.

We recall that one could also use the above mentioned space-time BIEs, hence the associated potential representations, also to restrict the original PDE exterior problem to a bounded region of physical interest. Indeed this approach could be used to construct transparent (or nonreflecting) boundary conditions on the boundary of the chosen region. Once these conditions have been determined, the solution of the original problem can be computed, in the new exterior bounded domain, by using standard numerical methods, such as, for example, finite differences or finite elements. In the last twenty years there has been an intensive research activity on this type of approach, and many papers have been published (see, for example,[12], [17], [23], [30] and their references).

In this paper, we consider the (2D and 3D) exterior problem for the non homogeneous wave equation, with a Dirichlet boundary condition and non homogeneous initial conditions. In particular, to solve this problem, in Section 2 we derive two alternative single-layer boundary integral equation formulations. Since the crucial point for the success of these formulations is the numerical evaluation of the "volume" integrals generated by the initial data, in Section 3 we propose an efficient numerical approach for their computation. In Section 4, we solve some test problems by applying a Lubich convolution quadrature for the discretization of the time integral, and a collocation first, and a Galerkin then, boundary element method. Finally, some conclusions are drawn in Section 5.

The main goals of the paper are the construction of an efficient numerical approach for the evaluation of the volume integrals and the numerical testing of a Lubich/BEM-collocation method for the solution of the proposed space-time BIE, since no stability and convergence (theoretical) results are known for this method.

As mentioned before, the particular behavior of the coefficients of the Lubich discrete convolution rules, which are used to discretize the time convolution integral, can

allow the costruction of fast solution methods, at least in the 3D Galerkin case. Moreover, as pointed out in [27], it appears that a significant saving can also be obtained in the potential evaluation, which would increase the efficiency of the overall approach, as a method for the solution of the original PDE problem. All these aspects will be examined in a forthcoming paper, where this approach will also be compared with those that are currently used within the absorbing (artificial) boundary condition strategy.

Before deriving our results, we briefly recall some known basic existence and uniqueness results on the PDE problems we are considering.

Let $\Omega^i \subset \mathbb{R}^d$ be an open bounded domain with a sufficiently smooth boundary Γ; define $\Omega^e = \mathbb{R}^d \setminus \bar{\Omega}^i$. By $C^m(I,F)$ we denote the set of C^m functions $f(x,t)$ of $t \in I$ valued in F, where $F = F(\Omega)$ is a Banach space. Given the functions $f \in C^m([0,T], H^{s-1}(\Omega^e))$ $m \geq 0$, $u_0 \in H^s(\Omega^e)$, $v_0 \in H^{s-1}(\Omega^e)$ and $g \in C([0,T], H^{s-1/2}(\Gamma))$ with $s \geq 1$ real, we consider the following Dirichlet problem for the wave equation:

$$\begin{cases} \Delta u(\mathbf{x},t) - u_{tt}(\mathbf{x},t) &= f(\mathbf{x},t) \quad \text{in } \Omega^e \times (0,T) \\ u(\mathbf{x},t) &= g(\mathbf{x},t) \quad \text{in } \Gamma \times (0,T) \\ u(\mathbf{x},0) &= u_0(\mathbf{x}) \quad \text{in } \Omega^e \\ u_t(\mathbf{x},0) &= v_0(\mathbf{x}) \quad \text{in } \Omega^e. \end{cases} \tag{1}$$

Since the boundary Γ is assumed smooth, the data f,u_0 and v_0 can be extended to $f \in C^m(\mathbb{R}, H^{s-1}(\mathbb{R}^d))$, $u_0 \in H^s(\mathbb{R}^d)$ and $v_0 \in H^{s-1}(\mathbb{R}^d)$, respectively (see [14]). Then we consider the associated problem

$$\begin{cases} \Delta u(\mathbf{x},t) - u_{tt}(\mathbf{x},t) &= f(\mathbf{x},t) \quad \text{in } \mathbb{R}^d \times \mathbb{R} \\ u(\mathbf{x},0) &= u_0(\mathbf{x}) \quad \text{in } \mathbb{R}^d \\ u_t(\mathbf{x},0) &= v_0(\mathbf{x}) \quad \text{in } \mathbb{R}^d. \end{cases} \tag{2}$$

This latter has a unique solution $\tilde{u} \in C^k(\mathbb{R}, H^{s-k}(\mathbb{R}^d))$ for each $k = 0, \cdots, m+2$ (see [33]). By subtracting (2) from (1) we obtain the following problem with null initial values

$$\begin{cases} \Delta u(\mathbf{x},t) - u_{tt}(\mathbf{x},t) &= 0 \quad \text{in } \Omega^e \times (0,T) \\ u(\mathbf{x},t) &= \bar{g}(\mathbf{x},t) \quad \text{in } \Gamma \times (0,T) \\ u(\mathbf{x},0) &= 0 \quad \text{in } \Omega^e \\ u_t(\mathbf{x},0) &= 0 \quad \text{in } \Omega^e, \end{cases} \tag{3}$$

where $\bar{g}(\mathbf{x},t) = g(\mathbf{x},t) - \tilde{u}(\mathbf{x},t)|_\Gamma$.

Remark 1.1 *If in (1) we further assume that the compatibility condition $g(\mathbf{x},0) = u_0(\mathbf{x})|_\Gamma$ is satisfied, then, since $\tilde{u}(\mathbf{x},0) = u_0(\mathbf{x})$ we also have $\bar{g}(\mathbf{x},0) = 0$.*

Notice that $\bar{g} \in C([0,T], H^{s-1/2}(\Gamma))$; therefore a natural extension of $\bar{g}$ for $t < 0$ and $t > T$ gives a distribution having the Laplace transform (with respect to the t variable) on $\mathbb{R}$ taking values (with respect to the space variable) in $H^{s-1/2}(\Gamma)$.

Following the notation introduced in [6], given a Banach space E we define:

$D'_+(E)$=$\{$distributions on $\mathbb{R}$ with values in E and null for $t < 0\}$
$S'_+(E)$=$\{$tempered distributions on $D'_+(E)\}$
$L'(E) = \{f \in D'_+(E) : e^{-\sigma_0 t} f \in S'_+(E)$ for some $\sigma_0 = \sigma_0(f) \in \mathbb{R}\}$
$H^k_\sigma(\mathbb{R}_+, E) = \{f \in L'(E) : e^{-\sigma t} \frac{\partial^k f}{\partial t^k} \in L^2(\mathbb{R}, E)\}$.

The following results have then been proved in [6] (see Theorems 1 and 2):
Given $\bar{g} \in L'(H^{1/2}(\Gamma))$, the exterior problem (3) has a unique solution in $L'(H^1(\Omega_e))$. Moreover, this has a unique single layer representation with density $\varphi \in L'(H^{-1/2}(\Omega^e))$. If furthermore $\bar{g} \in H^{3/2}_{\sigma_0}(\mathbb{R}_+, H^{1/2}(\Gamma))$ for a $\sigma_0 > 0$, then problem (3) has a unique solution $\bar{u} \in H^0_{\sigma_0}(\mathbb{R}_+, H^1(\Omega^e))$ that satisfies the following energy inequality:

$$\int_{-\infty}^{+\infty} e^{-2\sigma t} E_+(t) dt \leq C \frac{1}{\sigma^2} \max\left\{\frac{1}{\sigma_0}, 1\right\} \|\bar{g}\|^2_{\sigma,\frac{3}{2},\frac{1}{2}},$$

for each $\sigma \geq \sigma_0 > 0$, where

$$E_+(t) = \int_{\Omega^e} \Big(|\nabla \bar{u}(\mathbf{x}, t)|^2 + |\bar{u}_t(\mathbf{x}, t)|^2 \Big) d\mathbf{x}$$

and $\|\cdot\|_{\sigma,\frac{3}{2},\frac{1}{2}}$ is the norm of the space $H^{3/2}_{\sigma}(\mathbb{R}_+, H^{1/2}(\Gamma))$.

Remark 1.2 *Although in [6] the proof of this result was given only in the case $d = 3$, a careful reading of this proof shows that actually it holds also for $d = 2$.*

Thus, under the assumptions we have initially made, our original problem (1) has a unique solution $u = \bar{u} + \tilde{u} \in L'(H^1(\Omega^e))$. Unfortunately no regularity results, such as those given for problem (2) or for the interior case that we recall next, seem to be known for the exterior problem (1).

For the interior problem associated with (1) we have the following result, which has been proved in ([19], p.167; see however also [20]):
Let the boundary Γ be sufficiently smooth. Under the conditions

$$f \in L^1((0,T), H^m(\Omega^i)), \quad \frac{\partial^{m+1} f}{\partial t^{m+1}} \in L^1((0,T), L^2(\Omega^i))$$

$$u_0 \in H^{m+1}(\Omega^i), \quad v_0 \in H^m(\Omega^i), \quad \bar{g} \in H^{m+1}(\Gamma \times (0,T)),$$

m being a non negative integer, and assuming that all compatibility conditions (trace coincidence) that make sense are satisfied, the interior problem associated with (3) has a unique solution $u \in C([0,T], H^{m+1}(\Omega^i))$, with $\frac{\partial^{m+1} u}{\partial t^{m+1}} \in C([0,T], L^2(\Omega^i))$ and $\frac{\partial u}{\partial n_i} \in H^m(\Gamma \times (0,T))$.

The required degree of smoothness of Γ depends on the degree of regularity of the solution one wishes to obtain (see [14]). Moreover, with suitable definitions of fractional derivatives, the above result extends to the case $m = s$ non integer.

Here and in the following, $\partial_{n_e} = \frac{\partial}{\partial n_e}$ and $\partial_{n_i} = \frac{\partial}{\partial n_i}$ denote the outward (boundary) unit normal derivatives for the exterior and the interior problems, respectively.

2 Two space-time boundary integral equation formulations

To derive a single layer representation for problem (1), we consider the interior and exterior problems written in the form

$$\begin{cases} \Delta u(\mathbf{x},t) - u_{tt}(\mathbf{x},t) &= f(\mathbf{x},t) \quad \text{in}\,\Omega \times (0,T) \\ u(\mathbf{x},t) &= g(\mathbf{x},t) \quad \text{in}\,\Gamma \times (0,T) \\ u(\mathbf{x},0) &= u_0(\mathbf{x}) \quad \text{in}\,\Omega \\ u_t(\mathbf{x},0) &= v_0(\mathbf{x}) \quad \text{in}\,\Omega \end{cases} \tag{4}$$

where the domain $\Omega \subset \mathbb{R}^d,\ d = 2,3$ is either Ω^i or Ω^e. For simplicity we assume that the boundary Γ and the data satisfy the regularity and compatibility properties which guarantee the existence and uniqueness of the solutions of both problems in $C^2(\bar{\Omega} \times [0,T])$. We notice however that the numerical approach we will adopt in Section 4 to solve problems of type (4) requires the solution to be even smoother. We also assume that the data f, u_0, v_0 are defined in all of $\mathbb{R}^d$. This is not a restriction since, by assuming the required regularity of the boundary Γ, these data can always be smoothly extended to the interior domain. Moreover, as we shall point out at the end of the next section (see Remark 2.2), the potential representation does not depend on the chosen extension.

For our original exterior Dirichlet problem we will then be able to obtain two alternative integral equation formulations.

2.1 First BIE formulation

The basic machinery for deriving a BIE formulation is a classical one, and can be found in any textbook on PDE and boundary integral equations (see for example [10], [15]). Therefore we omit most of the mathematical details and briefly describe only the main steps.

One of the fundamental tools to obtain this representation is the well known Green's second formula, interpreted here in terms of generalized functions [34]. In our specific case, by considering the function G defined below, where $t > 0$ is arbitrary, for $\mathbf{x} \notin \Gamma$ this formula takes the following form:

$$\begin{aligned} &\int_\Omega \Delta u(\mathbf{y},s) G(\mathbf{x}-\mathbf{y},t-s)dy = \int_\Omega u(\mathbf{y},s)\Delta G(\mathbf{x}-\mathbf{y},t-s)d\mathbf{y} \\ &+ \int_\Gamma G(\mathbf{x}-\mathbf{y},t-s)\partial_n u(\mathbf{y},s)d\Gamma_{\mathbf{y}} - \int_\Gamma \partial_n G(\mathbf{x}-\mathbf{y},t-s)u(\mathbf{y},s)d\Gamma_{\mathbf{y}}. \end{aligned} \tag{5}$$

In the case we are examining $G(\mathbf{x},t)$ denotes the wave equation fundamental solution

$$\frac{\partial^2}{\partial t^2} G(\mathbf{x},t) - \Delta G(\mathbf{x},t) = \delta(\mathbf{x})\delta(t) \qquad (\mathbf{x},t) \in \mathbb{R}^d \times (0,T) \tag{6}$$

that is,

$$G(\mathbf{x},t)=\frac{1}{2\pi}\frac{H(t-\|\mathbf{x}\|)}{\sqrt{t^2-\|\mathbf{x}\|^2}},\qquad d=2,$$

$$G(\mathbf{x},t)=\frac{\delta(t-\|\mathbf{x}\|)}{4\pi\|\mathbf{x}\|}=\frac{\partial}{\partial t}\left[\frac{1}{4\pi\|\mathbf{x}\|}H(t-\|\mathbf{x}\|)\right]=:\frac{\partial}{\partial t}G_1(\mathbf{x},t),\qquad d=3.$$

$\delta(\cdot), H(\cdot)$ being the well known Dirac delta and Heaviside functions.

Remark 2.1 *In the 3D case, in the following we shall make use of the relationships:*

$$\int_0^{t+\varepsilon} v(\mathbf{y},s)G(\mathbf{x}-\mathbf{y},t-s)ds=\frac{\partial}{\partial t}\int_0^{t+\varepsilon} v(\mathbf{y},s)G_1(\mathbf{x}-\mathbf{y},t-s)ds,$$

$$\int_{\mathbb{R}^3} v(\mathbf{y})G(\mathbf{x}-\mathbf{y},t)d\mathbf{y}=\frac{\partial}{\partial t}\int_{\mathbb{R}^3} v(\mathbf{y})G_1(\mathbf{x}-\mathbf{y},t)d\mathbf{y}.$$

where $\varepsilon>0$ arbitrary and, in our cases, the functions v are smooth.

First we consider the interior problem and, having set $t^*=t+\varepsilon,\ \varepsilon>0$ as small as we like, define a C^2 extension of $u(\mathbf{y},s)$ in the interval $[0,t^*]$, such that $u(\mathbf{y},t^*)\equiv\frac{\partial}{\partial s}u(\mathbf{y},t^*)\equiv 0$. We multiply the wave equation by $G(\mathbf{x}-\mathbf{y},t-s)$ and integrate the resulting identity first on $(0,t^*)$ and then on Ω^i:

$$\begin{aligned}&\int_{\Omega^i}\int_0^{t^*} f(\mathbf{y},s)G(\mathbf{x}-\mathbf{y},t-s)dsd\mathbf{y} \qquad (7)\\ =\ &\int_{\Omega^i}\int_0^{t^*}\Delta u(\mathbf{y},s)G(\mathbf{x}-\mathbf{y},t-s)dsd\mathbf{y}-\int_{\Omega^i}\int_0^{t^*}\frac{\partial^2}{\partial s^2}u(\mathbf{y},s)\,G(\mathbf{x}-\mathbf{y},t-s)dsd\mathbf{y}.\end{aligned}$$

It can be easily shown that under the smoothness assumptions we have made on the solution $u(\mathbf{y},s)$, for the functions G defined above all integrals are well defined and the order of integration can be exchanged. We also notice, after performing integration by parts twice, that for any given $0<\|\mathbf{x}-\mathbf{y}\|\neq t$ we have:

$$\begin{aligned}&\int_0^{t^*}\frac{\partial^2}{\partial s^2}u(\mathbf{y},s)\,G(\mathbf{x}-\mathbf{y},t-s)ds\\ =\ &\int_0^{t^*}u(\mathbf{y},s)\frac{\partial^2}{\partial s^2}G(\mathbf{x}-\mathbf{y},t-s)ds-u_0(\mathbf{y})\frac{\partial}{\partial t}G(\mathbf{x}-\mathbf{y},t)-v_0(\mathbf{y})G(\mathbf{x}-\mathbf{y},t).\end{aligned}$$

Taking advantage of the Green's formula (5) and of identity (6), and treating properly the Ω-integration of the term containing the factor $\frac{\partial G}{\partial t}$ when using the last relationship, from (7) we obtain:

$$\begin{aligned}&\int_0^{t^*}\int_{\Omega^i}u(\mathbf{y},s)\delta(\mathbf{x}-\mathbf{y})\delta(t-s)d\mathbf{y}ds=\int_0^{t^*}\int_\Gamma G(\mathbf{x}-\mathbf{y},t-s)\partial_{n_i}u(\mathbf{y},s)\Gamma_{\mathbf{y}}ds\\ -\ &\int_0^{t^*}\int_\Gamma\partial_{n_i}G(\mathbf{x}-\mathbf{y},t-s)u(\mathbf{y},s)\Gamma_{\mathbf{y}}ds+\frac{\partial}{\partial t}\int_{\Omega^i}u_0(\mathbf{y})G(\mathbf{x}-\mathbf{y},t)d\mathbf{y}\\ +\ &\int_{\Omega^i}v_0(\mathbf{y})G(\mathbf{x}-\mathbf{y},t)d\mathbf{y}-\int_0^{t^*}\int_{\Omega^i}f(\mathbf{y},s)G(\mathbf{x}-\mathbf{y},t-s)d\mathbf{y}ds.\end{aligned}$$

Finally, by considering separately the cases $\mathbf{x} \in \Omega^i$ and $\mathbf{x} \in \Omega^e$, letting $\varepsilon \to 0$ we obtain the integral equation formulation for the interior problem:

$$\int_0^t \int_\Gamma G(\mathbf{x}-\mathbf{y}, t-s)\partial_{n_i} u(\mathbf{y}, s)\Gamma_{\mathbf{y}} ds - \int_0^t \int_\Gamma \partial_{n_i} G(\mathbf{x}-\mathbf{y}, t-s) u(\mathbf{y}, s)\Gamma_{\mathbf{y}} ds +$$
$$\frac{\partial}{\partial t}\int_{\Omega^i} u_0(\mathbf{y})G(\mathbf{x}-\mathbf{y}, t)d\mathbf{y} + \int_{\Omega^i} v_0(\mathbf{y})G(\mathbf{x}-\mathbf{y}, t)d\mathbf{y} - \int_0^t \int_{\Omega^i} f(\mathbf{y}, s)G(\mathbf{x}-\mathbf{y}, t-s)d\mathbf{y}ds$$
$$= \begin{cases} u(\mathbf{x}, t) & \mathbf{x} \in \Omega^i \\ 0 & \mathbf{x} \in \Omega^e. \end{cases} \tag{8}$$

Similarly, for the exterior problem we obtain:

$$\int_0^t \int_\Gamma G(\mathbf{x}-\mathbf{y}, t-s)\partial_{n_e} u(\mathbf{y}, s)\Gamma_{\mathbf{y}} ds - \int_0^t \int_\Gamma \partial_{n_e} G(\mathbf{x}-\mathbf{y}, t-s) u(\mathbf{y}, s)\Gamma_{\mathbf{y}} ds +$$
$$\frac{\partial}{\partial t}\int_{\Omega^e} u_0(\mathbf{y})G(\mathbf{x}-\mathbf{y}, t)d\mathbf{y} + \int_{\Omega^e} v_0(\mathbf{y})G(\mathbf{x}-\mathbf{y}, t)d\mathbf{y} - \int_0^t \int_{\Omega^e} f(\mathbf{y}, s)G(\mathbf{x}-\mathbf{y}, t-s)d\mathbf{y}ds$$
$$= \begin{cases} 0 & \mathbf{x} \in \Omega^i \\ u(\mathbf{x}, t) & \mathbf{x} \in \Omega^e. \end{cases} \tag{9}$$

The case $\mathbf{x} \in \Gamma$ needs to be treated more carefully, although also this situation can be handled in a fairly standard way (see for example [10]). It is sufficient to take the limits of the above representations as their interior point $\mathbf{x}$ approaches a point on the boundary Γ. A careful calculation gives again equations (8) and (9), where now $\mathbf{x} \in \Gamma$, both having however as right hand sides the quantity $\frac{1}{2}u(\mathbf{x}, t)$, i.e., $\frac{1}{2}g(\mathbf{x}, t)$.

Thus, summing the above integral formulations we finally obtain the single layer representation for our Dirichlet problem.

Formulation 1:

$$u(\mathbf{x}, t) = \int_0^t \int_\Gamma G(\mathbf{x}-\mathbf{y}, t-s)[\partial_n u(\mathbf{y}, s)]\Gamma_{\mathbf{y}} ds + \frac{\partial}{\partial t}\int_{\mathbb{R}^d} u_0(\mathbf{y})G(\mathbf{x}-\mathbf{y}, t)d\mathbf{y} \tag{10}$$
$$+ \int_{\mathbb{R}^d} v_0(\mathbf{y})G(\mathbf{x}-\mathbf{y}, t)d\mathbf{y} - \int_0^t \int_{\mathbb{R}^d} f(\mathbf{y}, s)G(\mathbf{x}-\mathbf{y}, t-s)d\mathbf{y}ds, \quad \mathbf{x} \in \Omega,$$

$$g(\mathbf{x}, t) = \int_0^t \int_\Gamma G(\mathbf{x}-\mathbf{y}, t-s)[\partial_n u(\mathbf{y}, s)]\Gamma_{\mathbf{y}} ds + \frac{\partial}{\partial t}\int_{\mathbb{R}^d} u_0(\mathbf{y})G(\mathbf{x}-\mathbf{y}, t)d\mathbf{y} \tag{11}$$
$$+ \int_{\mathbb{R}^d} v_0(\mathbf{y})G(\mathbf{x}-\mathbf{y}, t)d\mathbf{y} - \int_0^t \int_{\mathbb{R}^d} f(\mathbf{y}, s)G(\mathbf{x}-\mathbf{y}, t-s)d\mathbf{y}ds, \quad \mathbf{x} \in \Gamma,$$

where $[\partial_n u(\mathbf{y}, s)]$ denotes the normal derivative jump $[\partial_n u(\mathbf{y}, s)] = \partial_{n_e} u(\mathbf{y}, s) + \partial_{n_i} u(\mathbf{y}, s)$.

Remark 2.2 *Because of the presence of the Heaviside function in the expression defining the kernel G, each single formulation (8) and (9) requires the computation of volume integrals defined on the intersection of Ω with the disk/sphere of radius t centered at $\mathbf{x}$; a task that is by no means trivial. In the final formulation we have derived above, no matter what is the shape of the boundary Γ, the domain of integration of our volume integrals is a disk/sphere, which, as we shall show in Section 3, makes the integral*

calculation fairly simple. But in this case we have to assume, as we did, that all the problem data are defined (after a smooth extension, if needed) in the whole space $\mathbb{R}^d$.

We also point out that if one considers a different smooth extension of the data f, u_0, v_0 inside in the interior domain, although the corresponding known terms and unknown density in the above formulations would change, the associated potential $u(\mathbf{x}, t)$ would not change. This latter does not depend on the particular chosen extension.

2.2 Second BIE formulation

This formulation is a straightforward consequence of the introduction of the new unknown $\bar{u}(\mathbf{x}, t) = u(\mathbf{x}, t) - u_0(\mathbf{x}) - tv_0(\mathbf{x})$. This is the unique solution of the problem:

$$\begin{cases} \Delta\bar{u}(\mathbf{x},t) - u_{tt}(\mathbf{x},t) & = f(\mathbf{x},t) - \Delta u_0(\mathbf{x}) - t\Delta v_0(\mathbf{x}) & \text{in } \Omega \times (0,T) \\ \bar{u}(\mathbf{x},t) & = \bar{g}(\mathbf{x},t) & \text{in } \Gamma \times (0,T) \\ \bar{u}(\mathbf{x},0) & = 0 & \text{in } \Omega \\ \bar{u}_t(\mathbf{x},0) & = 0 & \text{in } \Omega, \end{cases} \tag{12}$$

where $\bar{g}(\mathbf{x}, t) = g(\mathbf{x}, t) - u_0(\mathbf{x})|_\Gamma - tv_0(\mathbf{x})|_\Gamma$. By proceeding as we did in the case of the previous formulation, it is very simple to obtain also the following alternative single layer representation:

Formulation 2:

$$\bar{u}(\mathbf{x},t) = \int_0^t \int_\Gamma G(\mathbf{x}-\mathbf{y}, t-s)[\partial_n \bar{u}(\mathbf{y},s)]\Gamma_{\mathbf{y}} ds + \int_0^t \int_{\mathbb{R}^d} \Delta u_0(\mathbf{y}) G(\mathbf{x}-\mathbf{y}, t-s) d\mathbf{y} ds$$
$$+ \int_0^t \int_{\mathbb{R}^d} s\Delta v_0(\mathbf{y}) G(\mathbf{x}-\mathbf{y}, t-s) d\mathbf{y} ds - \int_0^t \int_{\mathbb{R}^d} f(\mathbf{y},s) G(\mathbf{x}-\mathbf{y}, t-s) d\mathbf{y} ds, \quad \mathbf{x} \in \Omega.$$

$$\bar{g}(\mathbf{x},t) = \int_0^t \int_\Gamma G(\mathbf{x}-\mathbf{y}, t-s)[\partial_n \bar{u}(\mathbf{y},s)]\Gamma_{\mathbf{y}} ds + \int_0^t \int_{\mathbb{R}^d} \Delta u_0(\mathbf{y}) G(\mathbf{x}-\mathbf{y}, t-s) d\mathbf{y} ds$$
$$+ \int_0^t \int_{\mathbb{R}^d} s\Delta v_0(\mathbf{y}) G(\mathbf{x}-\mathbf{y}, t-s) d\mathbf{y} ds - \int_0^t \int_{\mathbb{R}^d} f(\mathbf{y},s) G(\mathbf{x}-\mathbf{y}, t-s) d\mathbf{y} ds, \quad \mathbf{x} \in \Gamma.$$

3 Computation of the "volume" integrals

We remark preliminarily that when the initial values u_0 and v_0 are such that $\Delta u_0 = \Delta v_0 = 0$, then the second integral formulation is the most convenient, since in this case it does not require the computation of the corresponding two "volume" integrals. Otherwise the first formulation should be preferred, since it requires only to use the data u_0, v_0, and not their Laplacians.

Therefore in this section we present an efficient numerical approach for the compu-

tation of integrals of the form

$$I_{u_0}(\mathbf{x},t) = \frac{\partial}{\partial t}\int_{\mathbb{R}^d} u_0(\mathbf{y})G(\mathbf{x}-\mathbf{y},t)d\mathbf{y} \tag{13}$$

$$I_{v_0}(\mathbf{x},t) = \int_{\mathbb{R}^d} v_0(\mathbf{y})G(\mathbf{x}-\mathbf{y},t)d\mathbf{y} \tag{14}$$

$$I_f(\mathbf{x},t) = \int_0^t \int_{\mathbb{R}^d} f(\mathbf{y},s)G(\mathbf{x}-\mathbf{y},t-s)d\mathbf{y}ds \tag{15}$$

with $\mathbf{x} \in \bar{\Omega}$, which appear in the first formulation.

We consider first the case $d = 2$. By introducing the polar coordinates, centered at $\mathbf{y} = \mathbf{x}$:

$$\mathbf{y} = \mathbf{x} + re_\theta, \qquad e_\theta = (\cos\theta, \sin\theta)^T$$

and recalling the definition of finite part integral (see [26]), here denoted by $\fint$, we have

$$I_{v_0}(\mathbf{x},t) = \frac{1}{2\pi}\int_0^{2\pi}\int_0^t \frac{1}{\sqrt{t-r}}\frac{rv_0(\mathbf{y})}{\sqrt{t+r}}drd\theta = \frac{t}{2\pi}\int_0^{2\pi}\int_0^1 \frac{1}{\sqrt{1-\xi}}\frac{\xi v_0(\mathbf{y}_t)}{\sqrt{1+\xi}}d\xi d\theta, \tag{16}$$

$$\begin{aligned} I_{u_0}(\mathbf{x},t) &= -\frac{t}{2\pi}\int_0^{2\pi} \fint_0^t \frac{ru_0(\mathbf{y})}{(t^2-r^2)^{3/2}}drd\theta = -\frac{t}{2\pi}\int_0^{2\pi} \fint_0^t \frac{1}{\sqrt{t-r}}\frac{\frac{ru_0(\mathbf{y})}{(t+r)^{3/2}}}{t-r}dr\ d\theta \\ &= -\frac{1}{2\pi}\int_0^{2\pi} \fint_0^1 \frac{1}{\sqrt{1-\xi}}\frac{\frac{\xi u_0(\mathbf{y}_t)}{(1+\xi)^{3/2}}}{1-\xi}d\xi\ d\theta, \end{aligned} \tag{17}$$

where we have set $\mathbf{y}_t = \mathbf{x} + t\xi e_\theta$. We recall (see [26]) that for our finite part integrals the change of variable is always allowed since the order of the hypersingularity is not integer.

Integral I_f is very similar to I_{v_0}, except for an extra integration:

$$\begin{aligned} I_f(\mathbf{x},t) &= \frac{1}{2\pi}\int_0^t\int_0^{2\pi}\int_0^{t-s} \frac{1}{\sqrt{(t-s)-r}}\frac{rf(\mathbf{y},s)}{\sqrt{t-s+r}}drd\theta ds \\ &= \frac{1}{2\pi}\int_0^t (t-s)\int_0^{2\pi}\int_0^1 \frac{1}{\sqrt{1-\xi}}\frac{\xi f(\mathbf{x}+(t-s)\xi e_\theta, s)}{\sqrt{1+\xi}}d\xi d\theta ds \\ &= \frac{t^2}{2\pi}\int_0^{2\pi}\int_0^1 \frac{1}{\sqrt{1-\xi}}\frac{\xi F(\mathbf{x},t;\theta,\xi)}{\sqrt{1+\xi}}d\xi d\theta \end{aligned} \tag{18}$$

where

$$F(\mathbf{x},t;\theta,\xi) = \int_0^1 (1-\eta)f(\mathbf{x}+t\xi(1-\eta)e_\theta, t\eta)d\eta, \tag{19}$$

In all cases the integration with respect to the θ variable will be performed using the classical trapezoidal rule. For the integration with respect to ξ we will proceed as follows. We consider the Gauss-Jacobi quadrature formula

$$\int_{-1}^1 \frac{1}{\sqrt{1-\chi}}\Psi(\chi)d\chi \approx \sum_{i=1}^k \lambda_i \Psi(\chi_i)$$

and map it onto the interval $(0,1)$:

$$\int_0^1 \frac{1}{\sqrt{1-\xi}}\Phi(\xi)d\xi \approx \frac{1}{\sqrt{2}}\sum_{i=1}^k \lambda_i \Phi(\xi_i)$$

where we have set $\xi_i = \frac{1+\chi_i}{2}$. Then we use this Gaussian formula for the inner integrals in I_{v_0} and I_f. For the corresponding finite part integral in I_{u_0} we use the Radau type Gaussian rule described in [25], that here takes the form:

$$\fint_0^1 \frac{1}{\sqrt{1-\xi}} \frac{\Phi(\xi)}{1-\xi} d\xi \approx a_0 \Phi(1) + \frac{1}{\sqrt{2}} \sum_{i=1}^{k} \frac{\lambda_i}{1-\xi_i}\ \Phi(\xi_i)$$

where

$$a_0 = -2 - \frac{1}{\sqrt{2}} \sum_{i=1}^{k} \frac{\lambda_i}{1-\xi_i} < 0.$$

The integral (19) can be computed using a classical Gauss-Legendre rule or a Gauss-Jacobi rule with weight $w(\eta) = 1 - \eta$.

To state a convergence result for the above product integration quadrature rules, we denote by $I(\mathbf{x}, t)$ either $I_{u_0}(\mathbf{x}, t)$ or $I_{v_0}(\mathbf{x}, t)$ or $I_f(\mathbf{x}, t)$, and by $Q(\mathbf{x}, t)$ the corresponding integration rules. The stepsize of the trapezoidal rule is denoted by h.

Theorem 3.1 *If $u_0, v_0, f \in C^{2\ell+1}(\mathbb{R}^d)$, then for any fixed m, n we have*

$$|I(\mathbf{x}_m, t_n) - Q(\mathbf{x}_m, t_n)| = O(k^{-2\ell-1}) + O(h^{2\ell+1}), \quad \ell \geq 0$$

in the case of $I_{v_0}(\mathbf{x}, t)$ or $I_f(\mathbf{x}, t)$, and

$$|I(\mathbf{x}_m, t_n) - Q(\mathbf{x}_m, t_n)| = O(k^{-2\ell}) + O(h^{2\ell+1}), \quad \ell \geq 1$$

in the case of $I_{u_0}(\mathbf{x}, t)$.

Proof. The above error estimates follows almost immediately from the well known error estimates for the trapezoidal rule and for the Gaussian formulas, and from the error bound given in ([25], Theorem 2.10). It is sufficient to compose these estimates as, for example, in ([25], Section 3.2). □

In the 3D case we introduce the spherical coordinates centered at $\mathbf{y} = \mathbf{x}$:

$$\mathbf{y} = \mathbf{x} + r e_{\theta,\phi}, \qquad e_{\theta,\phi} = (\cos\theta \sin\phi, \sin\theta \sin\phi, \cos\phi)^T.$$

Then, after some analytic manipulation we obtain the following expressions for our integrals I_{v_0} and I_{u_0}:

$$\begin{aligned} I_{v_0}(\mathbf{x}, t) &= \frac{1}{4\pi} \frac{d}{dt} \int_{r<t} \frac{v_0(\mathbf{y})}{r} d\mathbf{y} = \frac{1}{4\pi} \frac{d}{dt} \int_0^{\pi} \sin\phi\ d\phi \int_0^{2\pi}\ d\theta \int_0^t r v_0(\mathbf{x} + r e_{\theta,\phi}) dr \\ &= \frac{t}{4\pi} \int_0^{\pi} \sin\phi\ d\phi \int_0^{2\pi} v_0(\mathbf{x} + t e_{\theta,\phi})\ d\theta \end{aligned} \tag{20}$$

$$\begin{aligned} I_{u_0}(\mathbf{x}, t) &= \frac{1}{4\pi} \frac{d^2}{dt^2} \int_{r<t} \frac{u_0(y)}{r} d\mathbf{y} \\ &= \frac{1}{4\pi} \int_0^{\pi} \sin\phi\ d\phi \int_0^{2\pi} \left[u_0(\mathbf{x} + t e_{\theta,\phi}) + t \nabla u_0^T e_{\theta,\phi}\right]\ d\theta \end{aligned} \tag{21}$$

where, to simplify the notation, we have set $\nabla u_0 = \nabla u_0(\mathbf{x} + te_{\theta,\phi})$.

The above expression for I_{u_0} can be used if we have an analytic representation for $u_0(\mathbf{x})$. In this case ∇u_0 can be computed analytically. Otherwise we compute I_{u_0} using the following second order approximation:

$$\begin{aligned} I_{u_0}(\mathbf{x},t) &= \frac{d}{dt}\{\frac{t}{4\pi}\int_0^{\pi}\sin\phi\ d\phi\int_0^{2\pi}u_0(\mathbf{x}+te_{\theta,\phi})\ d\theta\} \\ &= \frac{I(t+h)-I(t-h)}{2h}+O(h^2) \end{aligned}$$

where we have set

$$I(t)=\frac{t}{4\pi}\int_0^{\pi}\sin\phi\ d\phi\int_0^{2\pi}u_0(\mathbf{x}+te_{\theta,\phi})\ d\theta. \tag{22}$$

Notice that in general the expressions given above for the computation of I_{u_0} and I_{v_0} require the knowledge of u_0 and v_0 at points lying outside the problem domain Ω. We recall however that we have assumed that the data are defined in all $\mathbb{R}^d$.

As for the 2D case, the expression for I_f is similar to that of I_{v_0}. Notice also that because of the particularly simple form of the 3D fundamental solution, the 3D volume final integral representations have the same dimensions of those we have in the 2D case.

In (20), (21) and (22) we propose to compute the integral over $(0,\pi)$ using the Gauss-Legendre quadrature rule; the integral over $(0,2\pi)$ can be evaluated efficiently by using the trapezoidal formula. For these rules too we can obtain error estimates like those in Theorem 3.1, first case.

Remark 3.2 *The success of the proposed approach, that is, the efficient computation of the volume integrals by means of the above quadratures with a low number of points, strongly depends on the behaviors of the functions u_0, v_0 and f within their domains of integration. If these behaviors are "nasty" or highly oscillatory, then one should use rules that take into account these behaviors or apply the above proposed rules with a sufficiently large number of nodes. See the case $T = 50$ in Example 1, Section 4.*

Finally, we recall that an integral of the form

$$\int_0^t\int_\Gamma G(\mathbf{x}-\mathbf{y},t-s)\varphi(\mathbf{y},s)d\Gamma_{\mathbf{y}}ds,\quad \mathbf{x}\in\Omega$$

which appears in our Formulations 1 and 2, can be computed using the Lubich time convolution quadrature (see [21]), coupled with a standard method for the integration over Γ.

4 The numerical solution of the single layer BIE

In this paper we consider smooth problems of form (4), i.e., problems defined on domains having a smooth boundary and smooth compatible data. For their solution we adopt the numerical approach which combine a second order (time) convolution quadrature of Lubich (see [21]) with a classical (nodal) collocation or Galerkin method (for the latter see [22]). In particular, for simplicity, in (4) we assume $f \in$

$C([0,T],C^2(\mathbb{R}^d))$, $u_0 \in C^3(\mathbb{R}^d)$, $v_0 \in C^2(\mathbb{R}^d)$ and the Dirichlet data $g \in C^2([0,T],C(\Gamma))$ satisfying the compatibility conditions:

$$g(\mathbf{x},0) = u_0(\mathbf{x})|_\Gamma, \qquad g_t(\mathbf{x},0) = v_0(\mathbf{x})|_\Gamma, \qquad g_{tt}(\mathbf{x},0) = \Delta u_0(\mathbf{x})|_\Gamma - f(\mathbf{x},0) \tag{23}$$

By adopting the first single layer formulation (11) we obtain the following boundary integral equation:

$$\int_0^t \int_\Gamma G(\mathbf{x}-\mathbf{y},t-s)[\partial_n u(\mathbf{y},s)]d\mathbf{y}ds = \bar{g}(\mathbf{x},t) \quad \mathbf{x} \in \Gamma, \tag{24}$$

where

$$\bar{g}(\mathbf{x},t) = g(\mathbf{x},t) - \frac{\partial}{\partial t}\int_{\mathbb{R}^d} u_0(y)G(\mathbf{x}-\mathbf{y},t)d\mathbf{y} - \int_{\mathbb{R}^d} v_0(\mathbf{y})G(\mathbf{x}-\mathbf{y},t)d\mathbf{y}$$
$$+\int_0^t \int_{\mathbb{R}^d} f(\mathbf{y},s)G(\mathbf{x}-\mathbf{y},t-s)d\mathbf{y}ds = g(\mathbf{x},t) - I_{u_0}(\mathbf{x},t) - I_{v_0}(\mathbf{x},t) + I_f(\mathbf{x},t).$$

For a result on the existence and uniqueness of the solution of (24) in a proper function space setting, see [6].

Assuming that the data of our problem (4) satisfy the above smoothness and compatibility conditions, which guarantee the existence of a classical (C^2) solution, in the next theorem we establish the corresponding smoothness and "compatibility" conditions for the function $\bar{g}(\mathbf{x},t)$ in (24).

Theorem 4.1 *Under the assumptions made above on the problem data we have $I_{u_0}, I_{v_0}, I_f \in C^2([0,T],C(\mathbb{R}^d))$. Moreover,*

$$\begin{array}{lll} I_{u_0}(\mathbf{x},0) = u_0(\mathbf{x}), & I'_{u_0}(\mathbf{x},0) = 0, & I''_{u_0}(\mathbf{x},0) = \Delta u_0(\mathbf{x}) \\ I_{v_0}(\mathbf{x},0) = 0, & I'_{v_0}(\mathbf{x},0) = v_0(\mathbf{x}), & I''_{v_0}(\mathbf{x},0) = 0 \\ I_f(\mathbf{x},0) = 0, & I'_f(\mathbf{x},0) = 0, & I''_f(\mathbf{x},0) = f(\mathbf{x},0) \end{array} \tag{25}$$

where $I' = \frac{d}{dt}I$, $I'' = \frac{d^2}{dt^2}I$; hence $\bar{g} \in C^2([0,T],C(\mathbb{R}^d))$ with

$$\bar{g}(\mathbf{x},0) = \bar{g}_t(\mathbf{x},0) = \bar{g}_{tt}(\mathbf{x},0) = 0. \tag{26}$$

Proof. Recalling identities such as (see [26]):

$$\frac{d}{dt}\int_0^t \frac{r^n h(\mathbf{y}_r)}{(t^2-r^2)^{1/2}}dr = -t \fint_0^t \frac{r^n h(\mathbf{y}_r)}{(t^2-r^2)^{3/2}}dr$$
$$\frac{d}{dt}\fint_0^t \frac{r^n h(\mathbf{y}_r)}{(t^2-r^2)^{m/2}}dr = -mt \fint_0^t \frac{r^n h(\mathbf{y}_r)}{(t^2-r^2)^{m/2+1}}dr, \quad n \geq 0, \quad m \geq 3$$

or, equivalently,

$$\frac{d}{dt}\fint_0^1 \frac{\xi^n}{(1-\xi^2)^{m/2}}h(\mathbf{x}+\alpha t\xi)d\xi = \fint_0^1 \frac{\xi^n}{(1-\xi^2)^{m/2}}\frac{d}{dt}h(\mathbf{x}+\alpha t\xi)d\xi, \quad n \geq 0,\ m \geq 3$$

and, for $n = 0$ and $m = 3, 5, 7, \dots$, odd integer,

$$\fint_0^1 \frac{d\xi}{(1-\xi^2)^{m/2}} d\xi = 0, \tag{27}$$

by performing Taylor expansions on $h(\mathbf{y}_r) = h(\mathbf{x} + re_\theta)$ and on $h(\mathbf{y}_r) = h(\mathbf{x} + re_{\theta,\phi})$, or on the corresponding $h(\mathbf{y}_t) = h(\mathbf{x} + t\xi e_\theta)$ and $h(\mathbf{y}_t) = h(\mathbf{x} + t\xi e_{\theta,\phi})$, after some lengthy and cumbersome calculation one obtains the results stated above.□

Remark 4.2 *Assume that the data of our problem are sufficiently smooth, to perform the required Taylor expansions, i.e., for example,*

$$f \in C^{\ell-2}([0,T], C^\ell(\mathbb{R}^d)),\ u_0 \in C^{\ell+1}(\mathbb{R}^d),\ v_0 \in C^\ell(\mathbb{R}^d),\ g \in C^\ell([0,T], C(\Gamma))$$

for some integer $\ell \geq 2$, and that they satisfy corresponding compatibility conditions of order up to $m \leq \ell$. Then, by means of the same machinery used to prove Theorem 4.1, one can easily show that $\bar{g} \in C^\ell([0,T], C(\mathbb{R}^d))$, with $\bar{g}(\mathbf{x}, 0) = \frac{d}{dt}\bar{g}(\mathbf{x}, 0) = \cdots = \frac{d^m}{dt^m}\bar{g}(\mathbf{x}, 0) = 0$.

Having shown that the right hand side of (24) satisfies (at least) the homogeneous compatibility conditions (26), we are now ready to solve (24) using a second order Lubich's discrete convolution rule.

Thus, for the numerical testing we consider Dirichlet problems of form (1), having initial/boundary conditions satisfying the compatibility contitions (23). In particular, we associate with them the following single layer BIE (see Formulation 1) :

$$\int_0^t \int_\Gamma G(\mathbf{x} - \mathbf{y}, t - s)\varphi(\mathbf{y}, s)\, d\Gamma_\mathbf{y}\, ds = g(\mathbf{x}, t) - I_{u_0}(\mathbf{x}, t) - I_{v_0}(\mathbf{x}, t) + I_f(\mathbf{x}, t) \tag{28}$$
$$\mathbf{x} \in \Gamma,\ t \in [0, T]$$

where the density function $\varphi(\mathbf{y}, s) = [\partial_n u(\mathbf{y}, s)]$ is sought on Γ, and I_{v_0}, I_{u_0} and I_f are defined by (16)-(21).

For its time discretization we split the interval $[0, T]$ into N steps of equal length $\Delta_t = T/N$ and collocate the equation at the discrete time levels $t_n = n\Delta_t$, $n = 0, \dots, N$:

$$\int_0^{t_n} \int_\Gamma G(\mathbf{x} - \mathbf{y}, t_n - s)\varphi(\mathbf{y}, s)\, d\Gamma_\mathbf{y}\, ds = g(\mathbf{x}, t_n) - I_{u_0}(\mathbf{x}, t_n) - I_{v_0}(\mathbf{x}, t_n) + I_f(\mathbf{x}, t_n) \tag{29}$$
$$\mathbf{x} \in \Gamma,\ n = 0, \dots, N.$$

The time integrals are then discretized by means of the Lubich convolution quadrature associated with the BDF method of order 2 (see [21]):

$$\sum_{j=0}^{n} \int_\Gamma \omega_{n-j}(\Delta_t; r)\varphi_{\Delta_t}(\mathbf{y}, t_j)\, d\Gamma_\mathbf{y}, \quad r = ||\mathbf{x} - \mathbf{y}||, \quad n = 0, \dots, N \tag{30}$$

whose coefficients ω_n are defined by

$$\omega_n(\Delta_t; r) = \frac{1}{2\pi\imath} \int_{|z|=\rho} K\left(r, \frac{\gamma(z)}{\Delta_t}\right) z^{-(n+1)}\, dz$$

where ρ is such that for $|z| \leq \rho$ the corresponding $\gamma(z)$ lies in the domain of analyticity of K, K is the Laplace transform of the fundamental solution G and $\gamma(z) = 3/2 - 2z + 1/2z^2$ is the characteristic quotient of the BDF method of order 2.

In the 2D case the Laplace transform K is defined by $K(r, z) = 1/(2\pi)K_0(rz)$, where K_0 denotes the modified Bessel function of the second kind of order 0, and in the 3D case by $K(r, z) = \exp(-rz)/(4\pi\, r)$.

By introducing the polar coordinate $z = \rho e^{\imath\varphi}$, the above integrals can be efficiently computed by a trapezoidal rule with L equal steps of length $2\pi/L$:

$$\omega_n(\Delta_t; r) \approx \frac{\rho^{-n}}{L} \sum_{l=0}^{L-1} K\left(r, \frac{\gamma(\rho \exp(\imath l 2\pi/L)}{\Delta_t}\right) \exp(-\imath n l 2\pi/L). \tag{31}$$

In this latter we choose $L = 2N$ and $\rho^N = \sqrt{\varepsilon}$, since Lubich in ([21]) has shown that this choice leads to an approximation of ω_n with relative error of size $\sqrt{\varepsilon}$, if K is computed with a relative accuracy bounded by ε. The choice of ε suggested by Lubich is 10^{-10}. According to the previous statement, this should give a relative accuracy of order 10^{-5}, which is sufficient for the tests we have performed and that we will present in the examples that will follow. All the ω_n are computed simultaneously by the FFT, with $O(N \log N)$ flops.

In the 3D case, instead of (31), for the computation of the ω_n we use a very simple three-term recurrence relation. By starting from the following alternative representation for ω_n (see [21]):

$$\omega_n(\Delta_t; r) = \frac{1}{n!} \frac{\partial^n}{\partial z^n} K\left(r, \frac{\gamma(z)}{\Delta_t}\right)\Big|_{z=0}, \qquad \gamma(z) = \sum_{i=1}^{k} \frac{1}{i}(1-z)^i$$

which holds for the Lubich's rules associated with the the k-step ($k \leq 6$) BDF method, having defined

$$v_n := \frac{\partial^n}{\partial z^n} \exp\left(-\frac{r}{\Delta_t}\gamma(z)\right)\Big|_{z=0}$$

in [27] we have obtained

$$\begin{cases} v_0 = \exp\left(-\dfrac{r}{\Delta_t}\gamma(0)\right) \\ v_{m+1} = -\dfrac{r}{\Delta_t} \displaystyle\sum_{\ell=0}^{m} \binom{m}{\ell} v_\ell \gamma^{(m+1-\ell)}(0), \ m = 0, 1, \ldots, n-1. \end{cases}$$

Then, setting

$$w_m = \frac{v_m}{m!}$$

the following final expressions

$$\begin{cases} w_0 = \exp\left(-\dfrac{r}{\Delta_t}\gamma(0)\right) \\ w_{m+1} = -\dfrac{r}{\Delta_t}\dfrac{1}{m+1} \displaystyle\sum_{\ell=0}^{m} w_\ell \frac{\gamma^{(m+1-\ell)}(0)}{(m-\ell)!}, \qquad m = 0, 1, \ldots, n-1 \end{cases}$$

and

$$\omega_n(\Delta_t; r) = \frac{w_n}{4\pi r}$$

hold for all the BDF methods. Notice however that, in the case of a k-step BDF method, $\gamma(z)$ is a polynomial of degree k and we have $\gamma^{(m+1-\ell)}(0) = 0$ whenever $m + 1 - l > k$. In particular, for the second order method we have

$$\gamma(0) = 3/2, \qquad \gamma^{(1)}(0) = -2, \qquad \gamma^{(2)}(0) = 1, \qquad \gamma^{(i)}(0) = 0,\ i > 2.$$

Thus in this case the above expression for w_{m+1} reduces to

$$\begin{cases} w_0 = \exp\left(-\dfrac{3r}{2\Delta_t}\right) \\ w_1 = 2\dfrac{r}{\Delta_t} w_0 \\ w_{m+1} = \dfrac{r}{\Delta_t}\dfrac{1}{m+1}\left(2w_m - w_{m-1}\right), \qquad m = 1, \ldots, n-1 \end{cases}$$

which is a minor variation of the corresponding representation obtained in [16].

By introducing the Lubich convolution quadrature rule (30) in (29) we have

$$\sum_{j=0}^{n} \int_\Gamma \omega_{n-j}(\Delta_t; r)\varphi^j_{\Delta_t}(\mathbf{y})\, d\Gamma_{\mathbf{y}} = g(\mathbf{x}, t_n) - I_{u_0}(\mathbf{x}, t_n) - I_{v_0}(\mathbf{x}, t_n) + I_f(\mathbf{x}, t_n) \tag{32}$$

$\mathbf{x} \in \Gamma,\ n = 0, \ldots, N$, where $\varphi^j_{\Delta_t}(\mathbf{y}) := \varphi_{\Delta_t}(\mathbf{y}, t_j)$.

For the space discretization, we employ standard collocation and Galerkin BEM, defined on quasiuniform boundary element meshes on Γ of (maximum) size Δ_x. In particular, in the 2D case first we assume that the curve Γ has a parametric representation $\mathbf{y} = \boldsymbol{\psi}(y)$. In this case the integration over Γ is reduced to an equivalent integration over a bounded interval, and the corresponding BEM approximant is defined by a (continuous) piecewise linear function associated with a uniform partition of this interval. Then we also consider the classical approach that approximates simultaneously, by polygonal functions defined on the same uniform mesh, the boundary Γ and the unknown $\varphi^j_{\Delta_t}(\mathbf{y})$. For simplicity, in the following, in both cases we denote by Γ the original boundary and its approximant. In the 3D case the surface Γ is approximated by that of a polyhedron having triangular faces; in this latter case the mesh width Δ_x is given by the maximum triangle diameter.

In all cases we denote the corresponding basis functions by $\{b_i(\mathbf{y})\}_{i=1}^M$, and the associated approximant by:

$$\varphi^n_{\Delta_t, \Delta_x}(\mathbf{y}) = \sum_{i=1}^{M} \varphi_{n\,i} b_i(\mathbf{y}), \qquad n = 0, \ldots, N$$

where, when $\mathbf{y} = \boldsymbol{\psi}(y)$, the notation $b_i(\mathbf{y})$ should be interpreted as $b_i(y)$.

Thus, the discrete problem consists of finding $\varphi^n_{\Delta_t, \Delta_x}(\mathbf{y})$, $n = 0, \ldots, N$ such that

$$\sum_{j=0}^{n}\sum_{i=1}^{M} \varphi_{j\,i} \int_\Gamma \omega_{n-j}(\Delta_t; ||\mathbf{x}_m - \mathbf{y}||) b_i(\mathbf{y})\, d\Gamma_{\mathbf{y}} = g(\mathbf{x}_m, t_n) - I_{u_0}(\mathbf{x}_m, t_n) - I_{v_0}(\mathbf{x}_m, t_n) + I_f(\mathbf{x}_m, t_n), \tag{33}$$

$m = 1, \ldots, M,\ n = 0, \ldots, N$ for the collocation BEM, and

$$\begin{aligned} &\sum_{j=0}^{n} \sum_{i=1}^{M} \varphi_{j\,i} \int_{\Gamma} \int_{\Gamma} \omega_{n-j}(\Delta_t; ||\mathbf{x} - \mathbf{y}||) b_i(\mathbf{y}) b_m(\mathbf{x})\, d\Gamma_{\mathbf{y}}\, d\Gamma_{\mathbf{x}} \\ &= \int_{\Gamma} \left[g(\mathbf{x}, t_n) - I_{u_0}(\mathbf{x}, t_n) - I_{v_0}(\mathbf{x}, t_n) + I_f(\mathbf{x}, t_n) \right] b_m(\mathbf{x})\, d\Gamma_{\mathbf{x}}, \end{aligned} \tag{34}$$

$m = 1, \ldots, M,\ n = 0, \ldots, N$ for the Galerkin BEM.

Both methods lead to a Toeplitz block lower triangular linear system of the form

$$\sum_{j=0}^{n} \mathbf{A}_{n-j} \boldsymbol{\varphi}_j = \mathbf{g}_n \qquad n = 0, \ldots, N \tag{35}$$

in the unknown vectors $\boldsymbol{\varphi}_j = (\varphi_{j\,1}, \ldots, \varphi_{j\,M})^T$, $j = 0, \ldots, n$. Since $\mathbf{A}_0$ turns out to be nonsingular, recalling that $g(\mathbf{x}, t_0) - I_{u_0}(\mathbf{x}, t_0) - I_{v_0}(\mathbf{x}, t_0) + I_f(\mathbf{x}, t_0) = \overline{g}(\mathbf{x}, 0) \equiv 0$ (see (26)), we further have $\boldsymbol{\varphi}_0 = \mathbf{0}$.

In the case of the Galerkin method, it has been proved (see [22]) that the matrix $\mathbf{A}_0$ is symmetric positive definite.

Remark 4.3 *The coefficients $\omega_{n-j}(\Delta_t; r)$ in (32) depend on $n - j$, not on n and j separately. This means that once we have constructed system (35), if we advance further in the time direction by the same stepsize Δ_t, we only need to construct the new matrix $\mathbf{A}_N$ and solve a new system of the form*

$$\mathbf{A}_0 \boldsymbol{\varphi}_{N+1} = \bar{\mathbf{g}}_{N+1}$$

where

$$\bar{\mathbf{g}}_{N+1} = \mathbf{g}_{N+1} - \sum_{j=1}^{N} \mathbf{A}_{N+1-j} \boldsymbol{\varphi}_j.$$

If however one wants to change Δ_t, then all the computation has to be restarted from $t = 0$.

Notice also that in the collocation case, the elements of the matrix $\mathbf{A}_0$, the only one that needs to be "inverted", are given by

$$(\mathbf{A}_0)_{mi} = \int_{\Gamma} \omega_0(\Delta_t; \|\mathbf{x}_m - \mathbf{y}\|) b_i(\mathbf{y}) d\Gamma_{\mathbf{y}},$$

where (see [27]), having set $r_m = \|\mathbf{x}_m - \mathbf{y}\|$, we have

$$\omega_0(\Delta_t; r_m) = \frac{1}{2\pi} K_0 \left(\frac{3}{2\Delta_t} r_m \right) \sim -\frac{1}{2\pi} \ln r_m,\ r_m \to 0$$

in the 2D case, $K_0(z)$ being the modified Bessel function of the second kind of order 0 (see [1]), and

$$\omega_0(\Delta_t; r_m) = \frac{1}{4\pi r_m} e^{-\frac{3}{2\Delta_t} r_m} \sim \frac{1}{4\pi r_m},\ r_m \to 0$$

in the 3D case. Therefore $\mathbf{A}_0$ is a classical collocation matrix for the single-layer BIE representation of the Dirichlet problem for the Helmholtz equation $\triangle u - s^2 u = 0$, with

wavenumber $s = 3/(2\Delta_t)$, defined on the (closed) curve/surface Γ. A similar remark applies also to the corresponding Galerkin matrix.

The mapping properties of the above mentioned single-layer representation, as well as the behaviors of corresponding Galerkin and collocation matrices, have been studied since many years. In particular in [6], in the 3D case the authors obtain an upper bound for the norm of the inverse of the single-layer operator, when this is acting between Sobolev spaces $(H^{-1/2},\ H^{1/2})$ which are suitable for the study and resolution of their variational formulation; this bound is of the form $C\Delta_t^{-1}$. Apparently it holds also for the 2D case, since its calculation relies on the Helmholtz equation but not on its dimension. In [5], [4] a nodal collocation method for the 2D case has been examined when the single-layer operator acts between proper Sobolev spaces (in our case: H^0, H^1), and corresponding error estimates have been derived. Moreover, a bound for the condition number of the $\mathbf{A}_0$ generated by our (piecewise linear) collocation method in the 2D case has been derived, when we assume Δ_t fixed and $M \to \infty$: this is $O(M)$. To our knowledge, till now a bound of this type has not been derived for the 3D case.

In spite of these results, in all the testing we have performed, where we simultaneously let $\Delta_t \to 0$ and $M \to \infty$, the (spectral) condition number of the matrix $\mathbf{A}_0$ has taken values close to 1 for $T = 1$, and fairly small for $T = 50$. In particular, in all the examples concerning the collocation method we had $cond_2(\mathbf{A}_0) \approx 1.5$ when $T = 1$, and $cond_2(\mathbf{A}_0) \approx 10$ for $T = 50$. Thus, in the cases we have examined the final linear system one has to solve appears to be well-conditioned. This seems to be due to the property that, in both the 2D and 3D cases, the coefficients $\omega_0(\Delta_t; r_m)$ defined above contains (see 9.7.2 in [1]) the factor $e^{-\frac{3}{2}\frac{r_m}{\Delta t}}$.

To determine the (relative) computational overhead due to the non homogeneous data, for the collocation method we notice that at each time step we have to compute two double integrals (I_{u_0}, I_{v_0}) and one triple integral (I_f). We remind that when the initial data u_0 is given in analytic form, from the computational point of view the 2D and 3D cases are very similar. For simplicity, we assume that in all cases each single integral is evaluated using a k-point rule. If the boundary discretization is defined by M grid points, the total number of function evaluations required by the volume integrals is $(2k^2 + k^3)M$. If one computes all elements of the M-order matrix A_n required to perform a new time step, then M^2 single integrals over Γ have to be evaluated. In the case of a piecewise linear approximant, the cheapest one, and assuming for simplicity that also these integrals are evaluated by means of an $k(k^2)$-point quadrature on each 1D (2D) boundary element where the test function is not the zero constant, the total computational cost is $2kM^2$ in the 2D case, and $\nu k^2 M^2$ in the 3D one, where $\nu \geq 3$ denotes the number of triangles having the same grid point as a vertex. Therefore, if M is sufficiently larger than k, the computational cost of the volume integrals becomes negligible with respect to that of a new matrix A_n. In any case, starting from $M \cong k^2/2 + k$ in the 2D case, and $M \cong k/\nu$ in the 3D case, the computational cost due to the volume integrals becomes smaller than that required by the construction of the associated matrix A_n, as M increases. About this point we remark that when the geometry of the boundary Γ is complex, M must necessarily take very large values, in particular when the boundary itself has to be approximated by a continuous piecewise linear function.

In the case of the Galerkin method, the overhead (rate) due to the volume integration at a first glance may appear higher, since each volume integral ought to be

integrated, with respect to the variable x, over the whole, albeit smooth, boundary Γ. But this is probably not the case, since to compute the matrix elements we have to perform an extra integration over each boundary element where its integrand function is not the zero constant. Nevertheless, since we are mainly concerned with the nodal collocation method, which is much faster, we will not examine further the Galerkin case. A remark about this point will be however made in Section 4, at the end of the first example.

To check the efficiency of the approach we have proposed to evaluate the volume integrals generated by the non homogeneous data, we have performed an intensive numerical testing, by solving several 2D and 3D problems. In Section 4 we will present two of them. In the 2D one, to test the stability and convergence of the method, in one case ($T = 1$) we have chosen $M = 2N$, while in the second one ($T = 50$) we set $M = N/2$; very similar convergence orders have been however obtained for $M = 2N, M = N, M = N/2$, and also for $M = N/16$.

We recall that for the corresponding Galerkin method, the convergence rate forecasted for the 3D case by the result in [22] is

$$\|\varphi(\cdot, t_n) - \varphi^n_{\Delta_t,\Delta_x}\|_{H^{-1/2}(\Gamma)} = O(\Delta_t^2) + O(\Delta_x^{5/2}), \tag{36}$$

uniformly with respect to $t_n \in [0, T]$. One obtains this bound by assuming, for example, in (24) $\bar{g} \in H^6((0, T), H^{1/2}(\Gamma))$ having all its derivatives up to order 4 vanishing at $t = 0$, and writing $\bar{g}$ as follows:

$$\bar{g}(\cdot, t) = \frac{\bar{g}^{(5)}(\cdot, 0)}{5!} t^5 + \bar{g}_1(\cdot, t).$$

Although a similar result has not been derived for the 2D case, this bound would suggest to take in both cases Δ_t and Δ_x such that $\Delta_t^2 \approx \Delta_x^{5/2}$ (see [16]), that is, $M \approx N^{4/5}$.

However, for simplicity, in our numerical testing we have preferred to compute a discrete L^2-norm of the errors produced by the proposed numerical method. In this case, since on the boundary of the space domain we define only quasiuniform meshes, and also taking into account a known inverse-type inequality for negative Sobolev norms (see, for example, [13]), it appears reasonable to conjecture, for the L^2-norm, a convergence rate of the type:

$$\|\varphi(\cdot, t_n) - \varphi^n_{\Delta_t,\Delta_x}\|_{L^2(\Gamma)} = O(\Delta_t^2) + O(\Delta_x^2).$$

Thus in the following two examples, we will apply a collocation method and verify if this expected quadratic rate of (unconditional) convergence holds. Since the above convergence estimate is uniform with respect to $t_n \in [0, T]$, we will examine the time pointwise behavior of the errors produced by the Lubich-collocation method.

Example 1

We consider first the 2D exterior Dirichlet problem (1) with the following data:

$$u_0(x_1, x_2) = \exp(-(x_1^2 + 2x_2^2)), \quad v_0(x_1, x_2) = \exp(-(2x_1^2 + x_2^2)),$$

$$f(x_1, x_2, t) = t^3 \exp(-(x_1^2 + x_2^2)),$$

$$g(x_1, x_2, t) = u_0(x_1, x_2) + tv_0(x_1, x_2) + \frac{t^2}{2}\Delta u_0(x_1, x_2),$$

where $t \in [0, T]$, $(x_1, x_2) \in \Gamma$ and Γ coincides with the boundary of the unit disk, parameterized by $(\cos(\theta), \sin(\theta))$, $\theta \in [-\pi, \pi)$. Notice that in this case data compatibility is guaranteed only up to order 2, i.e., for the associated function $\bar{g}(x, t)$ we only have $\bar{g}(x, 0) = \bar{g}_t(x, 0) = \bar{g}_{tt}(x, 0) = 0$. After having introduced the polar coordinates, we subdivide the interval $[-\pi, \pi)$ into M subintervals of equal length h_M, and choose as collocation points the abscissas $\theta_j = -\pi + jh_M$, $j = 0, 1, \ldots, M-1$, having set $\mathbf{x}_m = (\cos\theta_{m-1}, \sin\theta_{m-1})$, $m = 1 \ldots, M$.

In the testing reported in Table 1 the collocation matrix elements have been computed by applying a k-point Gauss-Legendre rule to each boundary element where the integrand is not identically equal to zero. The integrals I_{u_0}, I_{v_0} and I_f are evaluated using the quadrature rules described in Section 3. In particular, for the evaluation of the matrix elements, of I_{u_0} and I_{v_0}, we have chosen $k = 14$, while for that of I_f the choice $k = 6$ turns out to be sufficient. Notice that, depending on the accuracy one wants to achieve, a lower number of points could be sufficient. Indeed, higher values of k did not produce a better accuracy, while lower ones gave some loss of it.

To show the performance of the rules we have proposed to compute the volume integrals, in Figure 2 we have reported the values obtained in the case: $M = 16$, $N = 8$, $T = 1$. In particular we have reported the approximated values (reference values (k)) and the associated absolute estimated errors (absolute errors (k)) obtained by using k-point quadrature rules.

Figure 1: Example 1. $M = 16, N = 8, T = 1, t_n = 1$.

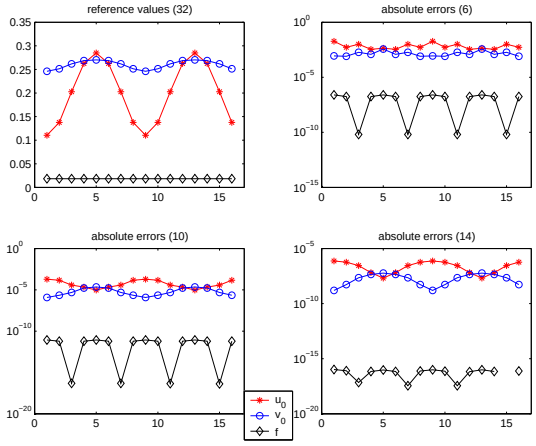

Since an analytic expression of the exact solution of the problem is not known, to determine these estimated errors we have taken as reference solution the approximant given by the method taking $N = 256$, $M = 512$ and computing all integrals using 32-point rules when $T = 1$, and 128-point rules for $T = 50$. An approximated density function: $(\theta, t) \to \varphi_{\Delta t, \Delta x}((\cos(\theta), \sin(\theta)), t)$ is plotted in Figure 2.

Figure 2: Example 1. Density function ($M = 32, N = 16$).

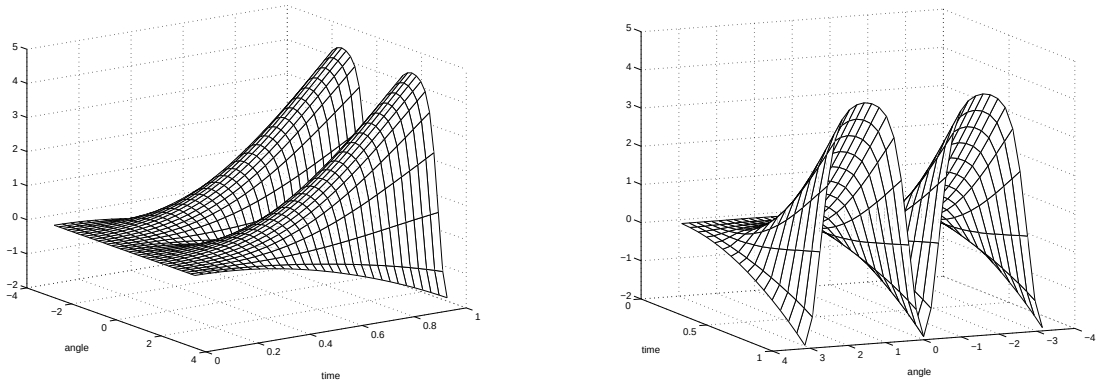

In Table 1 we have reported the ℓ^2-norm (estimated) relative errors

$$\left(\frac{h_M \sum_{m=1}^{M} [\varphi(x_m, t_n) - \varphi_{mn}]^2}{h_{512} \sum_{m=1}^{512} [\varphi(x_m, t_n)]^2} \right)^{1/2}$$

and the corresponding experimental convergence orders, obtained at the intermediate instants $t_n = 1/4, 1/2, 3/4$ and at $t_N = T = 1$ by using the collocation BEM. In the last column of the table we have reported the ratio (R_{CPU}) between the CPU time required by the evaluation of the known term $\mathbf{g}_n$ in (35), i.e. essentially that needed by the associated volume integrals, and the CPU time required by the construction of the matrix $\mathbf{A}_n$.

Table 1: Example 1. ℓ^2-norm relative errors, convergence order and CPU overhead.

M	N	$t_n = 1/4$	EOC	$t_n = 1/2$	EOC	$t_n = 3/4$	EOC	$t_N = 1$	EOC	R_{CPU}
16	8	$2.55E-01$		$7.40E-02$		$5.44E-02$		$6.09E-02$		0.13
			1.69		1.85		1.73		1.82	
32	16	$7.89E-02$		$2.05E-02$		$1.64E-02$		$1.72E-02$		0.06
			1.94		2.01		1.89		1.91	
64	32	$2.06E-02$		$5.11E-03$		$4.40E-03$		$4.57E-03$		0.03
			2.14		2.10		1.92		1.94	
128	64	$4.67E-03$		$1.19E-03$		$1.17E-03$		$1.20E-03$		0.013
			2.68		2.16		1.97		2.04	
256	128	$7.28E-04$		$2.66E-04$		$2.97E-04$		$2.91E-04$		0.007

To show that our numerical approach is equally efficient for larger values of T, we have applied the collocation method also to the case $T = 50$. The corresponding relative errors are reported in Table 2. Notice that the ratio R_{CPU} decreases as M increases; in particular, when we double the value of M, that of R_{CPU} appears to be halved.

To obtain these latter results, we have computed the matrix elements using 10-point rules, and the integrals I_{u_0} and I_{v_0} using 6-point rules. In this case the evaluation of I_f is more critical. For simplicity we have used a 64-point rule for each integral and for each time instant, although such a high number of points is excessive when t_n is significantly smaller that $T = 50$. A more efficient approach could be used, defined

Table 2: Example 1. ℓ^2-norm relative errors, convergence order and CPU overhead.

		$f \equiv 0$			$f \neq 0$		
M	N	$t_N = 50$	EOC	R_{CPU}	$t_N = 50$	EOC	R_{CPU}
16	32	$1.04E-01$		0.018	$7.12E-03$		67.3
			1.82			1.82	
32	64	$2.94E-02$		0.005	$2.02E-03$		30.8
			1.94			1.93	
64	128	$7.69E-03$		0.002	$5.30E-04$		14.6
			2.07			2.04	
128	256	$1.83E-03$		0.0009	$1.29E-04$		7.4

Figure 3: Example 1. $M = 16, N = 32, T = 50, t_n = 50$.

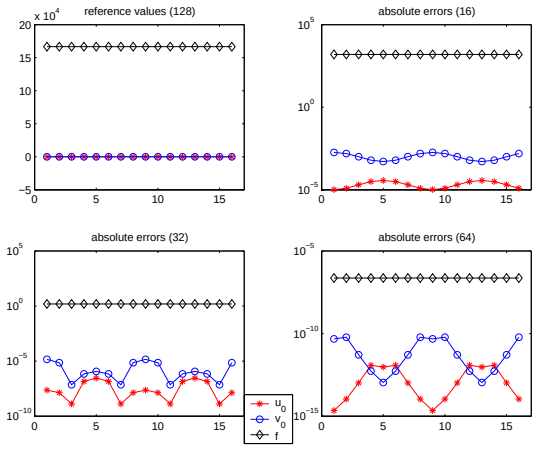

by the composition of basic k-point quadrature rules, with k low, which is refined as t_n increases; that is, having divided the interval $[0, T]$ into a (small) number of subintervals, when t_n moves from one of these to the next we refine the composition by adding one more copy of the rule. An approach of this type should reduce significantly the overhead index R_{CPU}.

We have also solved the same problem by approximating, as described above, the boundary Γ by a piecewise linear function, associated with the same mesh used to define the unknown $\varphi_{\Delta_t,\Delta_x}(y)$. The relative errors we have obtained differ from those reported in the tables below by negligible quantities.

Corresponding results have been obtained also for the Galerkin method. They are very similar to those given by the collocation method. However, in the Galerkin case, $T = 1$, to obtain these results we had to use a 33×32-point integration rule to compute the matrix elements, and a 32-point rule to evaluate the extra integration (over the boundary elements) of the known term.

Example 2

The next example we consider is the 3D Dirichlet problem (1) with data:

$$\begin{aligned} u_0(x_1,x_2,x_3) &= \exp(-(x_1+x_2+x_3)^2), \\ v_0(x_1,x_2,x_3) &= 2\sqrt{3}(x_1+x_2+x_3)\exp(-(x_1+x_2+x_3)^2), \\ f(x_1,x_2,x_3,t) &= 0, \\ g(x_1,x_2,x_3,t) &= \frac{t^3}{2\sqrt{\pi}} + \exp(-(x_1+x_2+x_3-\sqrt{3}t)^2), \quad t\in[0,T],\ (x_1,x_2,x_3)\in\Gamma \end{aligned}$$

$T=1$ and Γ coinciding with the boundary of the unit sphere. The problem data satisfy the compatibility conditions only up to order 2. The exact solution is such that in the above interval we have $[\partial_n u(\mathbf{x},t)] = \frac{3}{\sqrt{\pi}}t^2$.

Figure 4: Triangulation of the unit sphere for the discretization levels 2, 3 and 4.

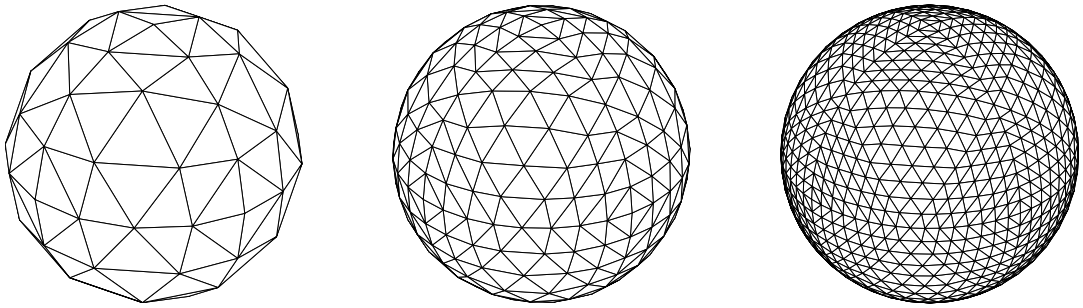

The time interval is divided into N instants. The space domain is approximated by the surface of a regular (inscribed) polyhedron having triangular faces (see Figure 2), obtained by using the algorithm contained in the software library BEMLIB, which can be downloaded from the internet site: http://bemlib.ucsd.edu (see [29]). In particular, for the refinement labeled level 1 we have 32 triangles and 18 vertices, at level 2: 128 triangles and 66 vertices, at level 3: 512 triangles and 258 vertices, and at level 4: 2048 triangles and 1026 vertices.

The integrals over each polyhedron triangular face, which define the matrix elements, are computed by introducing first the polar coordinates and then by applying the 12-point Gauss Legendre quadrature rule to each single integral. The computation of the integrals I_{u_0} and I_{v_0} has been performed using 14-point rules. In Table 3 we have reported the relative errors and the corresponding estimated convergence orders obtained at $t_n = 1/4, 1/2, 3/4, 1$, having chosen $t_N = T = 1$, and at the point $(1,0,0)$ since the solution, and its approximant, are constant for fixed t. We remind that the predicted error bound is uniform with respect to $t_n \in [0,T]$. Therefore, the error behaviors at $t_n = 3/4, 1$ should not be considered inconsistent.

In Table 4 the relative errors obtained taking $t_N = T = 50$ are listed. We recall that in this latter case we have

$$\varphi(\mathbf{x},t) = [\partial_n u(\mathbf{x},t)] = \frac{3}{\sqrt{\pi}} \sum_{k=0}^{\lfloor t/2 \rfloor} (t-2k)^2. \tag{37}$$

Thus, in this interval, the second order time derivative of φ is only piecewise continuous, having finite jumps at $t = 2, 4, \cdots, 50$.

Table 3: Example 2. Relative errors and experimental orders at $(1,0,0)$.

level	N	$t_n = 1/4$	EOC	$t_n = 1/2$	EOC	$t_n = 3/4$	EOC	$t_N = 1$	EOC	R_{CPU}
1	4	$4.55E-01$		$9.59E-02$		$3.75E-03$		$2.15E-02$		0.009
			1.63		2.29		1.11		1.58	
2	8	$1.47E-01$		$1.96E-02$		$1.74E-03$		$7.21E-03$		0.005
			2.02		1.74		1.37		3.23	
3	16	$3.62E-02$		$5.89E-03$		$6.74E-04$		$7.66E-04$		0.002
			1.96		1.80		0.99		4.40	
4	32	$9.31E-03$		$1.69E-03$		$3.39E-04$		$3.62E-05$		0.00001

Very similar relative errors have been obtained by performing the same testing on the previous problem, but with data $u_0 = 0,\ v_0 = 0,\ f = 0, g = \frac{t^3}{2\sqrt{\pi}}$, for which we still have the solution φ given by (37). This test case has been taken from [31]. We remark that the previous non homogeneous example has been derived from this simply by adding the wave equation solution $\exp(-(x_1 + x_2 + x_3 - \sqrt{3}t)^2)$, which is defined and smooth in $\mathbb{R}^3$. Thus the non homogeneous initial conditions have been properly treated.

Table 4: Example 2. Relative errors and experimental orders at $(1,0,0)$ for $t_N = 50$.

level	N	$t_N = 50$	EOC	R_{CPU}
1	32	$8.58E-02$		0.11
			1.68	
2	64	$2.68E-02$		0.03
			2.09	
3	128	$6.31E-03$		0.01

As noted in [16], many coefficients $\omega_n(\Delta_t; r)$ of Lubich's rule can be ignored, i.e. set equal to zero, since they are significant only in a neighborhood of $r/\Delta_t = t_n$. The introduction of such a modification reduces significantly the overall computational time, leaving unchanged the numerical solution accuracy.

Since the main goal of the paper is the application of Lubich's approach to problems having non homogeneous initial conditions, for simplicity in our testing we have not taken advantage of the fast solution techniques recently proposed, for example, in [16], [8]. For this reason, to solve this 3D problem we have not applied the Galerkin method.

All the numerical computation has been performed on a PC with two Intel Xeon® E5420 (2GHz) processors. We remark, however, that we have not considered the special features of our PC. To perform our numerical testing we have written standard (i.e., sequential) Matlab® codes.

5 Conclusion

In [22] Lubich, assuming certain smoothness and compatibility conditions, has proved that in the $3D$ case his approach combined with a space Galerkin method is unconditionally stable/convergent. Although this has not been explicitly derived for the $2D$ case, a similar result should hold also for this case. Indeed, all the fundamental results obtained in [6], and used by Lubich to derive his results, relies on properties of the Helmholtz equation which are independent from its dimension. Our numerical testing

seems to confirm this statement. In [16] a criteria for the selection of the discretization parameters required by this method have been discussed.

For the collocation method we have considered, there are no such results; those we have presented in Section 4 are only of experimental type. In the testing we have performed, the collocation method did not show any instability phenomenon; moreover, its accuracy and estimated convergence order appear to be very similar to those given by the Galerkin method.

All known theoretical results concerning Lubich's approach, as well as all those of experimental type (except for a few of them), deal with problems with homogeneous data. The main goal of our paper has been that of deriving mathematically a BIE representation in the non homogeneous case, to provide a simple integral representation for the associated volume integrals and very efficient quadrature rules for their evaluation. Therefore, the numerical testing we have performed has been tuned to check the efficiency of the proposed approach to evaluate the extra volume integrals, which does not depend on the shape of the space domain. In the case of a (smooth) domain very much different from a disc/sphere, the accuracy of the results and the computational cost would not change. Moreover, the accuracy we have obtained by solving the BIE in the non homogeneous case is very similar to that we had in the corresponding homogeneous case.

We remark that we had the expected rate of (unconditional) convergence also in situations where the data compatibility order was smaller than the one assumed in Lubich's theory.

Finally, we point out that if the time integration interval is not large, then the overhead due to the computation of the extra volume integrals generated by the non homogeneous data is either negligible or not superior to the computational cost required by the construction of the collocation matrix. We also remark that once the boundary integral equation has been solved, the potential evaluation can be performed by using very efficient quadrature formulas which are currently under investigation. It would then be interesting to compare this approach with the more standard finite element method, in particular when this is coupled with the construction of a (non reflecting) artificial boundary for the solution of exterior problems. In any case, the BIE approach appears to be more efficient when one has to compute the solution of the original PDE problem only in a small region of the (external) domain of integration.

Acknowledgement

The authors are grateful to the referees for their careful reading of the manuscript and their useful comments.

References

[1] M. Abramowitz and I. Stegun. *Handbook of Mathematical Functions*. National Bureau of Standards. A.M.S. 55, 1967.

[2] A.I. Abreu, W.J. Mansur, and A. Canelas. Computation of time and space derivatives in a cqm-based bem formulation. *Engineering Analysis with Boundary Elements*, 33:314–321, 2009.

[3] A.I. Abreu, W.J. Mansur, and J.A.M. Carrer. Initial conditions contribution in a BEM formulation based on the convolution quadrature method. *Internat. J. Numer. Methods Engrg.*, 67(3):417–434, 2006.

[4] S. Amini and S.M. Kirkup. Solution of helmholtz equation in the exterior domain by elementary boundary integral methods. *J. Comput. Phy.*, 118:208–221, 1995.

[5] D.N. Arnold and W.L. Wendland. On the asymptotic convergence of collocation methods. *Math. Comp.*, 41:197–242, 1983.

[6] A. Bamberger and T. Ha Duong. Formulation variationelle espace-temps pour le calcul par potentiel retardé de la diffraction d'une onde acoustique. *Math. Meth. in the Appl. Sci*, 8:405–435, 1986.

[7] A. Bamberger and T. Ha Duong. Formulation variationelle espace-temps pour le calcul par potentiel retardé de la diffraction d'une onde acoustique; Problème de Neumann. *Math. Meth. in the Appl. Sci*, 8:598–608, 1986.

[8] L. Banjai and S. Sauter. Rapid solution of the wave equation in unbounded domains. *SIAM J. Numer. Anal.*, 47(1):227–249, 2008.

[9] D.J. Chappell. A convolution quadrature Galerkin boundary method for the exterior Neumann problem of the wave equation. *Math. Meth. Appl. Sci.*, 32:1585–1608, 2009.

[10] D. Colton. *Partial Differential Equations: An Introduction*. Random House, New York, 1988.

[11] M. Costabel. Time-dependent problems with the boundary integral equation method. In*: Encyclopedia of Computational Mechanics* (E. Stein, R. de Borst, T.J.R. Hughes, eds). John Wiley Sons, New York, 2004.

[12] D. Givoli. *Numerical Methods for Problems in Infinite Domains*, volume 33. Studies in Applied Mechanics, Elsevier, Amsterdam, 1992.

[13] I.G. Graham, W. Hackbusch, and S. Sauter. Finite elements on degenerate meshes: inverse-type inequalities and applications. *IMA J. Numer. Anal.*, 25:379–407, 2005.

[14] P. Grisvard. *Elliptic Problems in Nonsmooth Domains*. Pitman, Boston - London, 1985.

[15] R.B. Guenther and J.W. Lee. *Partial Differential Equations of Mathematical Physics and Integral Equations*. Prentice-Hall, Inglewood Cliffs, NJ, 1988.

[16] W. Hackbusch, W. Kress, and S. Sauter. Sparse convolution quadrature for time domain boundary integral formulations of the wave equation. *IMA J. Numer. Anal.*, 29:158–179, 2009.

[17] T. Hagstrom. Radiation boundary conditions for numerical simulation of waves. *Acta Numer.*, 8:47–106, 1999.

[18] L. Kielhorn and M. Schanz. Convolution quadrature method-based symmetric Galerkin boundary element method for 3-d elastodynamics. *Internat. J. Numer. Methods Engrg.*, 76:1724–1746, 2008.

[19] I. Lasiecka, J.-L. Lions, and R. Triggiani. Nonhomogeneous boundary value problems for second order hyperbolic operators. *J. Math. Pures Appl.*, 65(2):149–192, 1986.

[20] J.-L. Lions and E. Magenes. *Problèmes aux limites non homogènes et applications*, volume 2. Dunod, Paris, 1968.

[21] Ch. Lubich. Convolution quadrature and discretized operational calculus. I. *Num. Math.*, 52:129–145, 1988.

[22] Ch. Lubich. On the multistep time discretization of linear initial-boundary value problems and their boundary integral equations. *Num. Math.*, 67(3):365–389, 1994.

[23] Ch. Lubich and A. Schädle. Fast convolution for nonreflecting boundary conditions. *SIAM J. Sci. Comput.*, 24(1):161–182, 2002.

[24] W.J. Mansur, D. Soares Jr., and M.A.C. Ferro. Initial conditions in frequency-domain analysis: the FEM applied to the scalar wave equation. *J. Sound and Vibration*, 270:767–780, 2004.

[25] G. Monegato. Numerical evaluation of hypersingular integrals. *J. Comput. Appl. Math.*, 50:9–31, 1994.

[26] G. Monegato. Definitions, properties and applications of finite part integrals. *J. Comput. Appl. Math.*, 229(2):425–439, 2009.

[27] G. Monegato, L. Scuderi, and M.P. Stanïc. Lubich convolution quadratures and their application to space-time BIEs. *Numer. Algorithms*, 2010, doi:10.1007/s11075-010-9394-9.

[28] W. Moser, H. Antes, and G. Beer. Soil-structure interaction and wave propagation problems in 2d by a duhamel integral based approach and the convolution quadrature method. *Comput. Mech.*, 36:431–443, 2005.

[29] C. Pozrikidis. *A Practical Guide to Boundary Element Methods with the Software Library BEMLIB.* Chapman & Hall/CRC, Boca Raton, Florida, 2002.

[30] D. Ruprecht, A. Schädle, F. Schmidt, and L. Zschiedrich. Transparent boundary conditions for time-dependent problems. *SIAM J. Sci. Comput.*, 30(5):2358–2385, 2008.

[31] S. Sauter and A. Veit. Solutions of time-domain boundary integral equations on the sphere. Construction and analytic properties. *Preprint, University of Zürich*, in preparation.

[32] M. Schanz, T. Rüberg, and L. Kielhorn. Time domain BEM: numerical aspects of collocation and Galerkin formulations. *in: Recent Advances in Boundary Element Methods (G.D. Manolis, D. Polyzos, eds.)*, pages 415–432, Springer Science, 2009.

[33] F. Treves. *Basic Linear Partial Differential Equations*, volume 62. Pure and Applied Mathematics, Academic Press, New York-London, 1975.

[34] V.S. Vladimirov. *Differential Equations of Mathematical Physics.* Dekker, New York, 1971.